https://doi.org/10.5194/egusphere-2026-1485
Preprint. Discussion started: 20 May 2026

Development of the CMA-GFS-AERO 4D-Var assimilation system v1.0- Part 2: Evaluation through cycling assimilation experiments

Chao Wang[1,2,3], Yongzhu Liu[1,2,3], Wei Han[1,2,3], Deying Wang[1,4], Xueshun Shen[1,2,3], Xiaoye Zhang[1,4]

[1]State Key Laboratory of Severe Weather Meteorological Science and Technology, Beijing, 10081, China
[2]CMA Earth System Modeling and Prediction Centre (CEMC), Beijing, 10081, China
[3]Key Laboratory of Earth System Modeling and Prediction, China Meteorological Administration, Beijing, 10081, China
[4]Chinese Academy of Meteorological Sciences, Beijing, 10081, China

Correspondence to: Yongzhu Liu (liuyzh@cma.gov.cn) and Wei Han (hanwei@cma.gov.cn)

Abstract. In Part 1 of this study (Liu et al., 2025), a strongly coupled aerosol–meteorology four-dimensional variational (4D-Var) data assimilation system, CMA-GFS-AERO 4D-Var, was developed based on the incremental analysis framework of the China Meteorological Administration Global Forecasting System (CMA-GFS), with black carbon (BC) selected as the initial assimilated aerosol species. In this second part, nearly three months of cycling data assimilation experiments from 10 October 2016 to 1 January 2017 were conducted to evaluate the practical performance of the system using BC surface observations from the China Atmosphere Watch Network (CAWNET). The impacts of BC assimilation on BC analyses, forecasts, and meteorological variables were systematically investigated. The results show that assimilating BC surface observations substantially improves the quality of both the BC background and analysis fields, with the analysis exhibiting a high degree of consistency with the observations. BC concentration forecasts are also significantly improved, particularly during severe pollution episodes over eastern China. The forecast benefits are mainly concentrated within the first 2–3 forecast days, with the largest improvements occurring during the initial 24 h forecast period. Moreover, assimilating BC surface observations yields a measurable positive impact on forecasts of near-surface 2 m air temperature (T2m) over heavily polluted regions, primarily through reductions in both warm and cold biases. These meteorological benefits are most pronounced during the early forecast period and gradually diminish with increasing forecast lead time. This study provides a comprehensive quantitative evaluation of the practical performance of CMA-GFS-AERO 4D-Var in real-data cycling assimilation experiments and demonstrates the effectiveness of strongly coupled aerosol–meteorology data assimilation in improving aerosol analyses and forecasts as well as meteorological predictions.

1 Introduction

Chemistry–meteorology interactions play a fundamental role in the atmospheric system through complex microphysical and radiative feedbacks. These feedbacks alter temperature, humidity, and atmospheric circulation, which subsequently affect the transport, transformation, and distribution of atmospheric chemical species (Seinfeld and Pandis, 1998; Gong et al., 2003; Guerrette and Henze, 2015). Coupled chemistry–meteorology models (CCMMs) therefore provide an important framework for jointly predicting atmospheric composition and weather (Zhang, 2008; Baklanov et al., 2014;

https://doi.org/10.5194/egusphere-2026-1485
Preprint. Discussion started: 20 May 2026

Bocquet et al., 2015). In recent years, data assimilation systems based on CCMMs have been increasingly developed to improve analyses and forecasts of aerosols and trace gases (Bocquet et al., 2015). Nevertheless, the impacts of chemical data assimilation on meteorological forecasts remain insufficiently investigated, particularly for aerosol assimilation and near-surface meteorological variables.

Several studies have explored the application of four-dimensional variational (4D-Var) data assimilation within CCMMs. At the European Centre for Medium-Range Weather Forecasts (ECMWF), aerosol and chemically reactive gases assimilation systems have been developed within the Integrated Forecast System (IFS) framework (Engelen et al., 2009; Benedetti et al., 2009; Inness et al., 2009, 2013, 2015). Previous studies demonstrated that assimilating aerosol and trace gas observations can significantly improve analyses and forecasts of atmospheric composition (Mangold et al., 2011; Inness et al., 2009). In addition to improvements in atmospheric composition, several studies also reported impacts of chemical data assimilation on meteorological fields. For instance, Semane et al. (2009) showed that assimilating ozone observations in the ARPEGE/MOCAGE (Action de Recherche Petite Échelle Grande Échelle / Modèle de Chimie Atmosphérique de Grande Échelle) system reduces wind biases in the lower stratosphere, while Ménard et al. (2019) further demonstrated that assimilating long-lived chemical species can improve zonal wind forecasts in the tropical lower stratosphere.

These studies have laid a solid foundation for the development of data assimilation in CCMMs. Nevertheless, most existing systems adopt a weakly coupled configuration, in which the tangent-linear and adjoint models of meteorology and chemistry are integrated separately within the 4D-Var inner loop (Inness et al., 2009). In addition, adjoint coupling between chemical tracers and the wind field through the tracer continuity equation is often disabled (Inness et al., 2015). As a consequence, chemical observations influence primarily the composition fields, with little or no feedback on meteorological analyses and forecasts. Accordingly, previous evaluations have largely focused on improvements in aerosol and trace gas distributions, whereas systematic assessments of the impacts on meteorological forecasts remain limited. Moreover, studies that do examine meteorological responses to chemical data assimilation have mainly emphasized trace gas observations and their effects on stratospheric dynamics. In contrast, the meteorological impacts of aerosol assimilation—particularly on near-surface variables—have received comparatively little attention.

Strongly coupled meteorology–chemistry data assimilation offers a practical approach for investigating the impacts of chemical data assimilation on atmospheric variables. In Part 1 of this study (Liu et al., 2025), we developed a strongly coupled aerosol–meteorology data assimilation system, CMA-GFS-AERO 4D-Var, focusing on strongly absorbing black carbon (BC) aerosols, which are known to exert pronounced radiative effects (Chung and Seinfeld, 2002; Menon et al., 2002; Bond et al., 2013). In this system, the tangent-linear and adjoint models of meteorology and aerosols are fully coupled, allowing BC observations to directly influence atmospheric analyses through aerosol–meteorology interactions.

https://doi.org/10.5194/egusphere-2026-1485
Preprint. Discussion started: 20 May 2026

While Part 1 primarily focused on the formulation, development, and validation of the system using idealized experiments, its practical performance in real-data cycling assimilation and its impacts on aerosol and meteorological forecasts have not yet been comprehensively evaluated.

In this second part, we conducted real-data cycling assimilation experiments over a nearly three-month period, assimilating BC surface observations using the CMA-GFS-AERO 4D-Var system. The impacts of BC assimilation on the quality of BC background and analysis fields were systematically assessed. In addition, a severe air pollution episode was selected to further examine the impacts of BC assimilation on the forecast performance of BC concentrations and key meteorological variables, with particular attention to near-surface meteorological conditions. The results of this study provide a comprehensive assessment of the CMA-GFS-AERO 4D-Var system, highlighting the role of strongly coupled aerosol–meteorology 4D-Var data assimilation in improving forecasts of aerosols and meteorological variables. The following text is divided into four sections. Section 2 briefly introduces the CMA-GFS-AERO 4D-Var system, Sect. 3 describes the setup of the cycling assimilation experiments and data, Sect. 4 presents the results, and the conclusions are found in Sect. 5.

2 Description of the CMA-GFS-AERO 4D-Var system

The CMA-GFS-AERO 4D-Var is a strongly coupled aerosol–meteorology four-dimensional variational data assimilation system recently developed by the CMA Earth System Modeling and Prediction Centre (CEMC) to investigate the influence of aerosol data assimilation on meteorological forecasts (Liu et al., 2025). The system is based on the incremental 4D-Var framework of the China Meteorological Administration Global Forecasting System (CMA-GFS; Zhang et al., 2019), which serves as the meteorological core of the coupled system. In CMA-GFS-AERO 4D-Var, a BC aerosol module (AERO-BC) is interactively coupled with the CMA-GFS weather model in an online framework. The coupled model represents major BC aerosol processes, including emissions, transport, hygroscopic growth, coagulation, condensation, dry deposition/sedimentation, and below-cloud scavenging. To support four-dimensional variational data assimilation, tangent linear and adjoint versions of the coupled aerosol–meteorology model were further developed, forming the dynamical core of the strongly coupled 4D-Var system.

The assimilation system uses BC mass concentration together with atmospheric variables as control variables. BC surface observations are assimilated through an observation operator that converts model variables into observation-equivalent quantities and interpolates them to observation locations. The background error covariance of the control variable BC is represented using prescribed horizontal and vertical correlation structures and evolves implicitly within the assimilation window through the tangent linear model dynamics, thereby generating flow-dependent cross-variable error correlations between BC and meteorological fields. Through the fully coupled tangent linear and adjoint models, BC observations can influence atmospheric analyses via aerosol–meteorology interactions.

The CMA-GFS-AERO 4D-Var system adopts a 6 h cycling assimilation framework with four assimilation windows per day

https://doi.org/10.5194/egusphere-2026-1485
Preprint. Discussion started: 20 May 2026

(03:00–09:00, 09:00–15:00, 15:00–21:00, and 21:00–03:00 UTC). In each cycle, the outer loop integrates the nonlinear coupled model to generate the trajectory and observation innovations, while the inner loop performs minimization using the tangent linear and adjoint models. Additional technical details regarding the model formulation, tangent linear and adjoint development, observation operator, and background error covariance are provided in Part 1 of this study (Liu et al., 2025).

3 Experimental setup and data

3.1 Experimental setup

We evaluated the performance of the CMA-GFS-AERO 4D-Var system using cycling data assimilation experiments conducted over a nearly three-month period from 10 October 2016 to 1 January 2017. The control experiment (BC_CTRL) assimilated only atmospheric observations, with types and usage identical to those employed in the operational CMA-GFS 4D-Var system (see Table S1 in Part 1 of this study). The second experiment (BC_CAWNET) assimilated both atmospheric observations and BC surface measurements, as described in Section 3.2.1. A summary of the experimental design is provided in Table 1.

Table 1. Design of the cycling data assimilation experiments.

Experiments	Period	Description
BC_CTRL	10 Oct. 2016 – 1 Jan. 2017	Assimilation of operational meteorological observations only
BC_CAWNET	10 Oct. 2016 – 1 Jan. 2017	Assimilation of operational meteorological and BC surface observations

Apart from the assimilated variables, all other configurations were identical between the two experiments. The CMA-GFS-AERO 4D-Var experiments employed a dual-resolution configuration, with the outer-loop forward integration performed at 0.25° horizontal resolution using a 300 s time step, while the inner-loop minimization utilized the tangent linear and adjoint models at 1.0° resolution with a 900 s time step. The model configuration included 87 vertical levels extending up to approximately 0.1 hPa. In the variational minimization procedure, only one outer loop was conducted, and the maximum number of inner-loop iterations was limited to 50. This configuration was found to provide stable convergence in the cycling assimilation experiments.

The CMA-GFS-AERO forecasts were initialized at 03:00 UTC on 1 October 2016 and restarted every 6 h. For each assimilation cycle, the meteorological initial conditions were taken from the operational CMA-GFS analysis fields. The BC field was initialized with zero concentrations at the beginning of the experiment and subsequently cycled using the BC forecast fields from the previous cycle. The first 9 d of the simulation was treated as a spin-up period and excluded from the analysis. Based on the analysis fields obtained from these cycling experiments, additional forecast experiments were conducted for the selected heavy pollution episode to evaluate the impact of BC assimilation on BC forecast performance and the feedback on

https://doi.org/10.5194/egusphere-2026-1485
Preprint. Discussion started: 20 May 2026

atmospheric variables, as detailed in Section 4.

3.2 Data

3.2.1 BC surface observations

BC observations were obtained from the China Atmosphere Watch Network (CAWNET), which has conducted BC measurements across China since 2006 (Xu et al., 2020). The dataset used in this study includes measurements from 32 stations consisting of 11 urban, 17 rural, and 4 remote sites (Guo et al., 2020). The spatial distribution of these stations is shown in Fig. S2 in Part 1 of this study (Liu et al., 2025). BC mass concentrations were measured using AE31 Aethalometers (Magee Scientific, USA, https://www.aerosolmageesci.com). In this study, BC concentrations at the wavelength of 880 nm were used. The original 5 min observations were quality controlled to remove abnormal and instrument-flagged records, followed by the generation of hourly averaged BC concentrations for assimilation and evaluation.

3.2.2 MERRA-2 BC reanalysis data

The second Modern-Era Retrospective analysis for Research and Applications (MERRA-2) is the latest atmospheric reanalysis data produced by NASA Global Modeling and Assimilation Office (GMAO) and was released in 2017 (Randles et al., 2017). Built upon the Goddard Earth Observing System Model Version 5 (GEOS-5) data assimilation system, MERRA-2 assimilates a wide range of satellite and surface observations of aerosol optical depth (AOD), including retrievals from Moderate Resolution Imaging Spectroradiometer (MODIS), Advanced Very High Resolution Radiometer (AVHRR), and Multiangle Imaging SpectroRadiometer (MISR), as well as direct measurements from the ground-based Aerosol Robotic Network (AERONET). Aerosol processes in MERRA-2 are simulated using the Goddard Chemistry, Aerosol, Radiation and Transport model (GOCART), which treats the sources, sinks, and chemistry of various aerosol components such as dust, sea salt, black and organic carbon, and sulfate. MERRA-2 provides continuous global coverage from 1980 to the present at a horizontal resolution of 0.5° × 0.625°, with 72 vertical levels. Its temporal products are available at 1-hourly, 3-hourly, and monthly intervals. In this study, we use the monthly surface BC mass concentration from the MERRA-2 product.

3.2.3 BC emissions

Anthropogenic BC emissions used in this study were derived from several emission inventories, including the Multi-resolution Emission Inventory for China (MEIC; Li et al., 2017; Zheng et al., 2018), the Copernicus Atmosphere Monitoring Service global and regional emissions (CAMS; Granier et al., 2019), and the global datasets of the Task Force Hemispheric Transport of Air Pollution (HTAP; Janssens-Maenhout et al., 2015). These datasets were processed into gridded emission fields using the EMIPS emission source processing system (Chen et al., 2023). The extracted BC emissions were then used as input for the CMA-GFS-AERO model simulations.

https://doi.org/10.5194/egusphere-2026-1485
Preprint. Discussion started: 20 May 2026

4 Results

4.1 Evaluation of the cycling BC data assimilation

4.1.1 BC analysis performance

We first conducted a sanity check using the BC mass concentrations from both the background and the analysis over the period from 10 October 2016 to 1 January 2017 to assess the performance of the analysis against the assimilated observations. A successful analysis is expected to yield smaller departures from the observations than the background, indicating better statistical agreement with the assimilated data (Benedetti et al., 2009). Figure 1 depicts scatterplots of assimilated BC observations versus background (Fig.1a) and analysis (Fig. 1b). Visually, the analysis exhibits less scatter than the background. Statistically, the analysis achieves a higher correlation coefficient (R=0.84) and a lower root mean square error (RMSE=2.53) compared to the background (R=0.71, RMSE=3.29), confirming the good performance of the analysis.

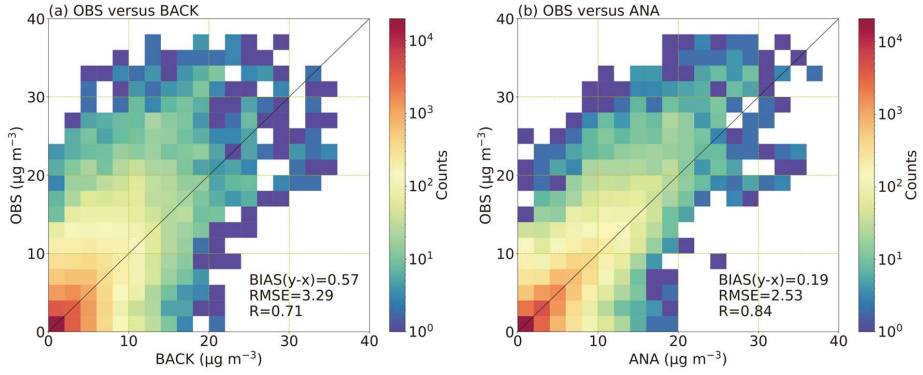

Figure 1. Scatterplots of CAWNET BC observations versus (a) background and (b) analysis BC concentrations from 10 October 2016 to 1 January 2017. Each panel shows the density distribution of hourly BC concentrations, with a total of 47,349 data points.

We further evaluated the performance of BC data assimilation cycling in the two experiments by examining the observation-minus-background (OMB) and observation-minus-analysis (OMA) statistics. Figure 2 shows the time series of 24-h averaged bias and root mean square (RMS) of BC OMB and OMA for both experiments, spatially averaged over CAWNET BC stations, from 10 October 2016 to 1 January 2017. As shown in Fig. 2a, the OMB and OMA bias curves of the BC_CTRL cycling assimilation experiment almost overlap, with only very minor differences. This behavior is expected, as BC_CTRL does not assimilate BC observations but only assimilates meteorological observations, which have limited impact on the BC analysis field. This result is also consistent with the findings in Part 1 of this study (Liu et al., 2025). The mean values of the OMB and OMA bias for the BC_CTRL experiment are both 1.8 μg m^{-3}. In contrast, the OMB bias curve of the BC_CAWNET cycling assimilation experiment is clearly closer to the zero line than that of BC_CTRL, with a mean value of 0.5 μg m^{-3}, representing

https://doi.org/10.5194/egusphere-2026-1485
Preprint. Discussion started: 20 May 2026

a bias reduction of approximately 72%. This indicates that assimilating surface BC observations from CAWNET substantially improves the BC background field. Furthermore, the OMA bias curve of BC_CAWNET is even closer to zero than its OMB, with a mean value of 0.2 μg m^{-3}, suggesting a very good agreement between the analysis and the observations.

Similar characteristics are observed in the RMS statistics shown in Fig. 2b. The OMB and OMA RMS curves of the BC_CTRL cycling assimilation experiment nearly coincide, with mean values of 3.6 μg m^{-3} for both. For the BC_CAWNET cycling assimilation experiment, the OMB RMS curve lies below that of BC_CTRL, with a mean value of 3.0 μg m^{-3}, indicating a reduced departure from observations in the background field. The OMA RMS curve of BC_CAWNET remains the lowest among all RMS curves during the entire period, with a mean value of 2.3 μg m^{-3}, demonstrating a further improvement in the analysis field after assimilating BC observations.

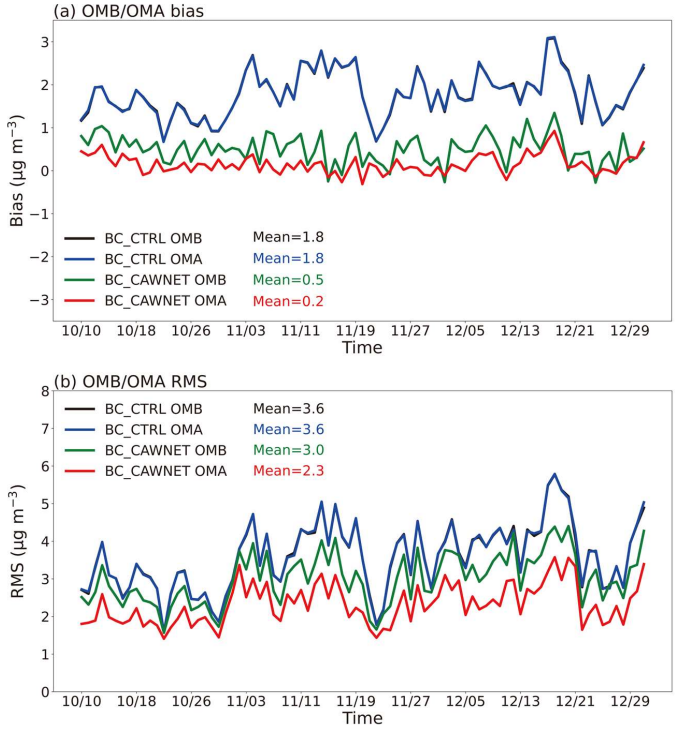

Figure 2. Time series of 24-h averaged (a) bias and (b) RMS of BC OMB and OMA, spatially averaged over CAWNET BC stations, for the BC_CTRL and BC_CAWNET cycling experiments from 10 October 2016 to 1 January 2017.

To assess the performance of BC assimilation across China, six representative stations from the CAWNET network were selected to ensure both geographical coverage and environmental diversity. These stations cover North China, Northeast China, Northwest China, East China, and Southwest China, and include urban, rural, and remote sites. Detailed information on the

https://doi.org/10.5194/egusphere-2026-1485
Preprint. Discussion started: 20 May 2026

selected stations is summarized in Table 2. Figure 3 presents the time series of 24-h averaged BC concentrations from observations, background, and analysis at the six stations for the BC_CTRL and BC_CAWNET cycling experiments from 10 October 2016 to 1 January 2017. In the BC_CTRL cycling assimilation experiment, the temporal variations of BC concentrations in both the background and analysis fields generally follow the observed trends at urban stations (Fig.3a-d), while at rural (Fig.3e) and remote (Fig.3f) stations, both the background and analysis fields fail to capture the detailed fluctuation patterns of the observations. In addition, the simulated concentrations are substantially underestimated compared to the observations at all sites. In contrast, in the BC_CAWNET cycling assimilation experiment, the background fields exhibit much closer agreement with the observations in both temporal variability and concentration magnitude. Correspondingly, the statistical metrics, including R and RMSE, show significant improvement relative to the BC_CTRL experiment. Furthermore, the analysis fields in the BC_CAWNET experiment demonstrate an even closer correspondence with the observations than the background fields. The correlation coefficients at all six stations are close to 0.9, with values reaching as high as 0.99 at Zhengzhou (Fig.3b), Chengdu (Fig.3c), and Gaolanshan (Fig.3e) station. Meanwhile, the RMSE values are reduced by approximately half or more compared to those in the BC_CTRL experiment. These results indicate that assimilating BC surface observations substantially improves both background and analysis BC concentrations, with robust performance across different regions and site types in China.

Table 2. Detailed information on six representative stations from CAWNET.

Stations	Latitude	Longitude	Region	Type
Beijing	39.8°N	116.47°E	North China	Urban
Zhengzhou	34.78°N	113.68°E	North China	Urban
Chengdu	30.65°N	104.04°E	Southwest China	Urban
Fushun	41.88°N	123.95°E	Northeast China	Urban
Gaolanshan	36°N	105.85°E	Northwest China	Rural
Lin'an	30.3°N	119.73°E	East China	Remote

https://doi.org/10.5194/egusphere-2026-1485
Preprint. Discussion started: 20 May 2026

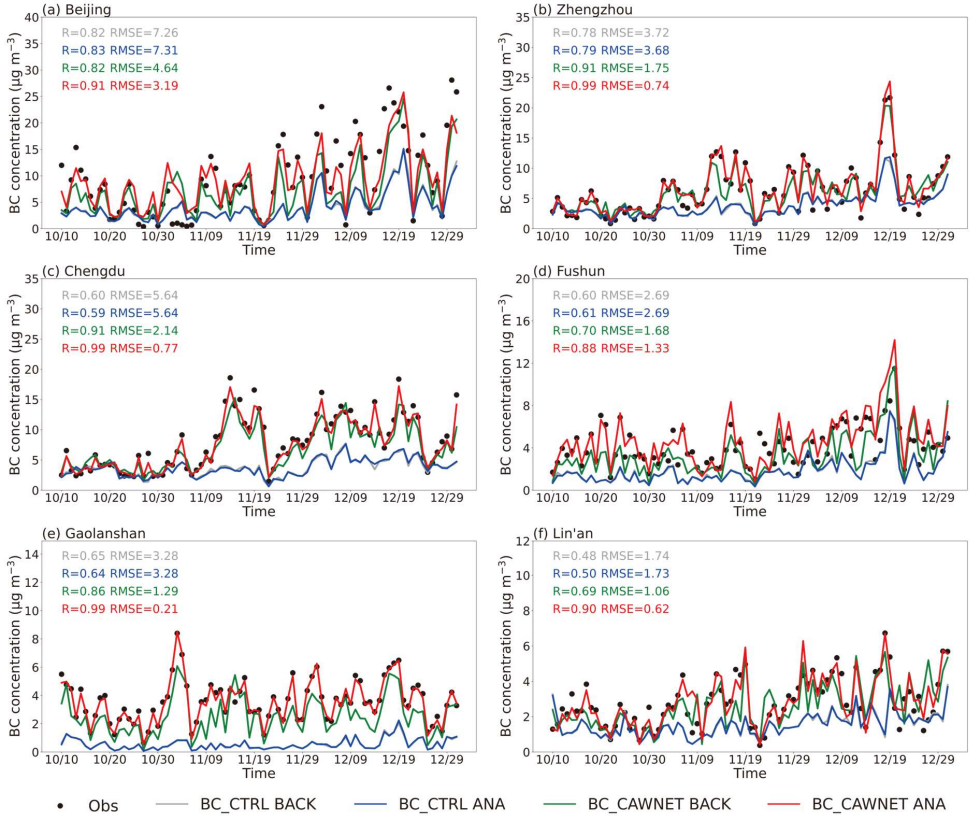

Figure 3. Time series of 24-h averaged BC concentrations from observations (Obs), background (BACK), and analysis (ANA) at (a) Beijing, (b) Zhengzhou, (c) Chengdu, (d) Fushun, (e) Gaolanshan, and (f) Lin'an stations for the BC_CTRL and BC_CAWNET cycling experiments from 10 October 2016 to 1 January 2017.

215

4.1.2 Independent evaluation with MERRA-2 reanalysis

Figure 4 shows the mean BC surface concentrations in the analysis fields from the BC_CTRL and BC_CAWNET cycling experiments, as well as from the MERRA-2 reanalysis, averaged over November and December 2016. The BC_CTRL cycling experiment generally reproduces the large-scale spatial contrast of higher BC concentrations in eastern China and lower values

220 in western China; however, it severely underestimates BC concentrations over eastern China, with maximum values of only about 4 μg m^{-3}. In contrast, the BC_CAWNET cycling experiment effectively captures the high BC concentration features over northeastern, eastern, and southwestern China, with peak values exceeding 8 μg m^{-3}. Both the spatial distribution and the magnitude of BC surface concentrations in the BC_CAWNET experiment are much closer to those in the MERRA-2 reanalysis. Note that, as the BC_CAWNET experiment assimilated only BC observations within China, BC levels over India are only

225 partially represented.

These results indicate that, after assimilating BC surface observations, the analysis fields produced by the BC_CAWNET

https://doi.org/10.5194/egusphere-2026-1485
Preprint. Discussion started: 20 May 2026

cycling experiment exhibit substantial improvements in both spatial distribution and concentration magnitude. Consistent with the comparison against CAWNET observations discussed in the previous section, the BC_CAWNET experiment shows markedly better agreement with the MERRA-2 reanalysis than the BC_CTRL experiment, effectively correcting the systematic underestimation of BC surface concentrations over eastern China. The locations and intensities of high-BC regions are also more realistically represented. As MERRA-2 data are not assimilated in this study, this comparison provides an independent validation, demonstrating that the assimilation of BC surface observations imposes stronger constraints on the model and significantly enhances the reliability and robustness of the analyzed BC fields.

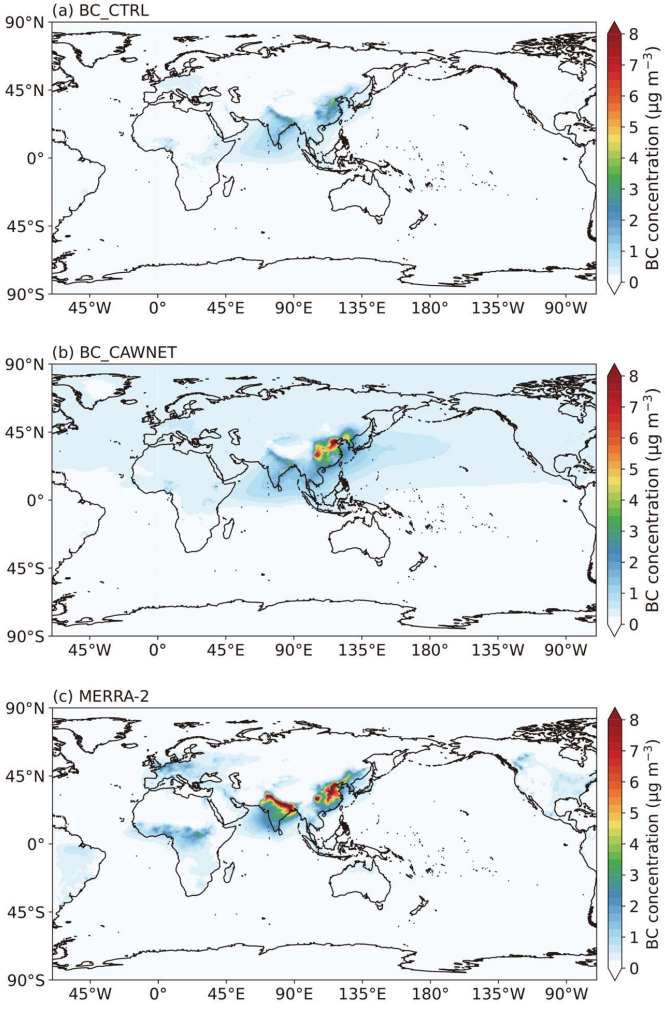

Figure 4. Spatial distribution of mean BC surface concentration in November and December 2016 from the analyses of (a) BC_CTRL, (b) BC_CAWNET, and (c) MERRA-2.

https://doi.org/10.5194/egusphere-2026-1485
Preprint. Discussion started: 20 May 2026

4.2 Impacts of BC assimilation on forecast performance

While Section 4.1 evaluated the performance of the cycling BC data assimilation in reproducing observed BC concentrations, this section further examines the impacts of BC assimilation on BC forecast performance and its feedback on meteorological variables during a severe air pollution episode. From 16 to 22 December 2016, eastern China experienced a heavy pollution event with persistently elevated BC concentrations. Additional forecast experiments were therefore conducted for this period to assess the influence of BC assimilation on subsequent forecasts. The forecasts were initialized from the analysis fields of the BC_CTRL and BC_CAWNET cycling experiments, respectively. Forecasts were launched twice daily at 00:00 and 12:00 UTC from 16 to 22 December 2016, with a forecast length of 120 h and without further data assimilation. Apart from the initial conditions, all model configurations were kept identical between the two forecast experiments.

4.2.1 Impacts on BC forecasts

Figure 5 compares the forecasted BC surface concentrations over eastern China initialized at 00:00 UTC on 19 December 2016 from the BC_CTRL and BC_CAWNET experiments at forecast lead times of 6, 12, 24, 48, and 72 h. For reference, the corresponding BC analysis fields from the BC_CAWNET cycling experiment at the same valid times are also shown. This case corresponds to the pollution peak and is used to illustrate the spatial differences between the two experiments and their evolution with forecast lead time. Overall, the BC_CTRL forecasts generally underestimate BC concentrations, with smaller and weaker high-concentration areas compared to the BC_CAWNET analysis. In contrast, the BC_CAWNET forecasts show substantial improvements in both the spatial extent and magnitude of high BC concentrations, closely matching the BC_CAWNET analysis throughout most of the forecast period.

At short lead times (6–24 h), the BC_CTRL forecasts capture the general spatial pattern of BC distribution but substantially underestimate peak concentrations, with maximum values of about 15 μg m^{-3}. In contrast, the BC_CAWNET forecasts reproduce the contiguous high-concentration areas over the North China Plain, including Beijing, Tianjin, Hebei, Shandong, and Henan, with peak values reaching approximately 30 μg m^{-3}, showing good agreement with the BC_CAWNET analysis. This indicates that BC assimilation effectively corrects the underestimated initial BC concentration and enables a realistic representation of both the intensity and spatial continuity of severe BC pollution during the early forecast period.

At 48 h lead time, the BC_CTRL forecasts show a markedly weakened and spatially confined high-concentration region, limited mainly to southern Hebei, with peak values of about 15 μg m^{-3}. The BC_CAWNET forecasts, however, retain more extensive high-BC regions covering Beijing, Tianjin, southern Hebei, and northern Henan, with peak concentrations reaching approximately 20 μg m^{-3}. The BC_CAWNET analysis further indicates that elevated BC concentrations persist over a broader area, including Beijing, Tianjin, southern Hebei, western Shandong, and southern Henan, with maximum values of around 25 μg m^{-3}. These results demonstrate that BC assimilation helps preserve both the spatial extent and magnitude of severe pollution at the medium forecast range, whereas the BC_CTRL forecasts exhibit a premature weakening and spatial contraction of high-

https://doi.org/10.5194/egusphere-2026-1485
Preprint. Discussion started: 20 May 2026

BC regions.

At 72 h lead time, the BC_CTRL and BC_CAWNET forecasts, together with the BC_CAWNET analysis, exhibit consistent spatial patterns, while the severe pollution over the North China Plain has largely dissipated, with only residual high-concentration areas remaining over Shandong. Despite the similar spatial distribution, differences in magnitude remain, with the BC_CTRL forecast producing the weakest concentrations (approximately 10–15 μg m^{-3}), followed by the BC_CAWNET forecast (around 15 μg m^{-3}), and the highest concentrations shown in the BC_CAWNET analysis (approximately 15–25 μg m^{-3}). This indicates that, although the influence of the initial BC concentrations weakens and forecasts initialized from different conditions tend to converge at longer lead times, BC assimilation continues to exert a positive impact on BC concentration magnitude, yielding a modest improvement in reproducing peak values.

https://doi.org/10.5194/egusphere-2026-1485
Preprint. Discussion started: 20 May 2026

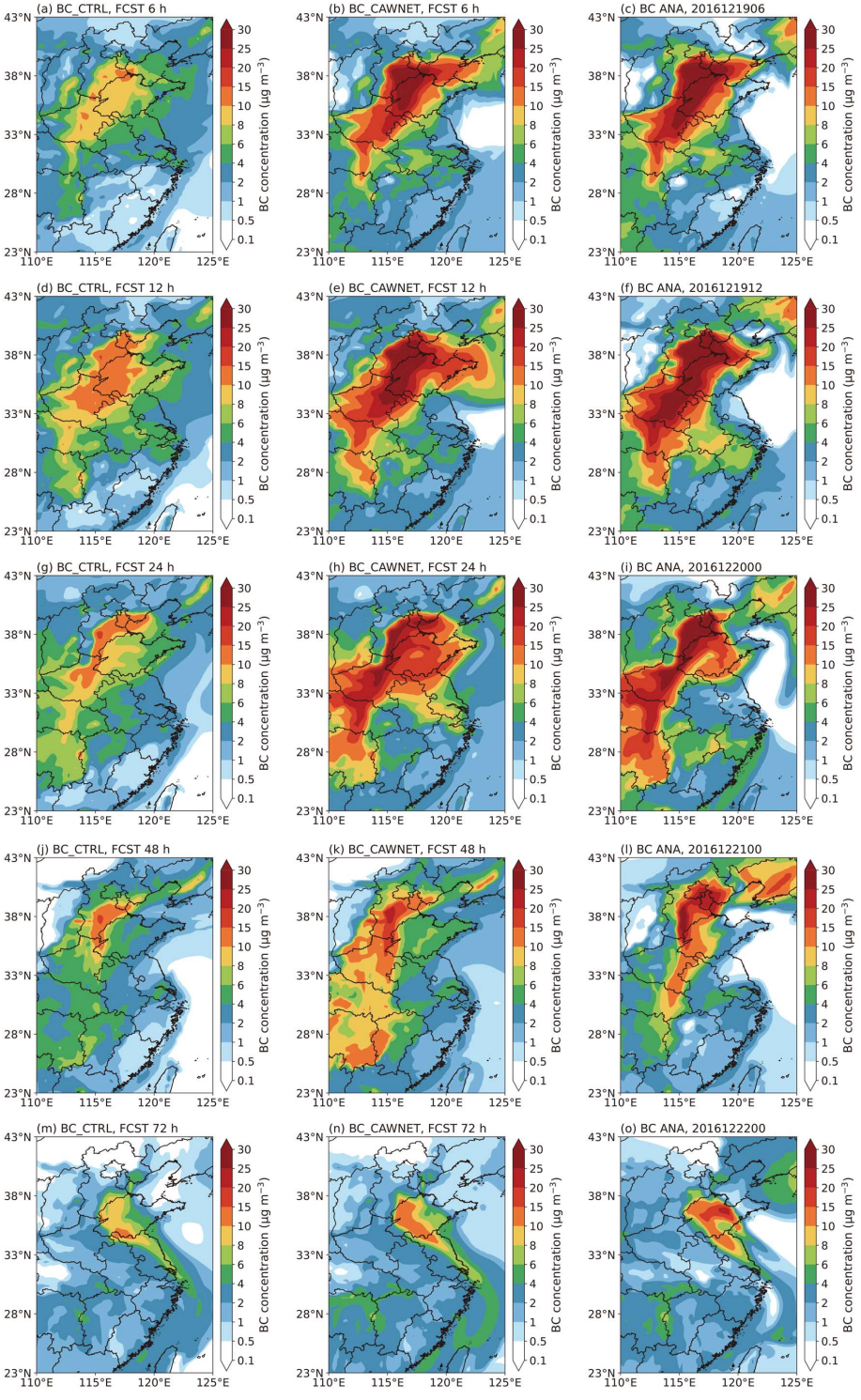

280

Figure 5. Spatial distributions of BC surface concentration forecasts over eastern China, initialized at 00:00 UTC on

https://doi.org/10.5194/egusphere-2026-1485
Preprint. Discussion started: 20 May 2026

19 December 2016 from the BC_CTRL (left column) and BC_CAWNET (middle column) experiments at forecast lead times of 6, 12, 24, 48, and 72 h (from top to bottom). The corresponding BC analysis fields from the BC_CAWNET cycling experiment at the same valid times are shown in the right column.

Figure 6 provides a quantitative evaluation of BC surface concentration forecast errors through the time series of BC observation-minus-forecast (OMF) bias and RMS averaged over CAWNET stations for the BC_CTRL and BC_CAWNET forecasts initialized at 00:00 UTC on 19 December 2016. As shown in Fig. 6a, the OMF bias of the BC_CTRL forecast is predominantly negative throughout the forecast period, indicating a systematic underestimation of BC surface concentrations. This underestimation is particularly pronounced during approximately the first two days of the forecast, which corresponds to the severe BC pollution episode over eastern China (Fig. 5), suggesting that the BC_CTRL forecast inadequately represents high-concentration pollution events. Averaged over the full 120 h forecast period, the mean OMF bias of the BC_CTRL forecast reaches −2.7 μg m⁻³. In contrast, the OMF bias of the BC_CAWNET forecast is substantially closer to zero during approximately the first two days of the forecast, demonstrating a clear improvement attributable to BC assimilation. This improvement is closely associated with a more realistic representation of spatially contiguous high-concentration regions over the North China Plain, as shown in Fig. 5. At longer lead times (beyond 72 h), the OMF bias curves of the BC_CTRL and BC_CAWNET forecasts converge and nearly overlap, indicating that the influence of the initial BC concentrations gradually weakens. Over the full 120 h forecast period, the mean OMF bias of the BC_CAWNET forecast is −1.8 μg m⁻³, corresponding to a bias reduction of approximately 33% relative to the BC_CTRL forecast. Consistent results are found for the OMF RMS (Fig. 6b). Compared with the BC_CTRL forecast, the BC_CAWNET forecast exhibits systematically lower RMS values, with the largest reduction occurring during the same early forecast period. As the forecast lead time increases, the RMS curves of the two forecasts progressively converge. Averaged over the full 120 h forecast period, the mean OMF RMS decreases from 5.4 μg m⁻³ for the BC_CTRL forecast to 4.5 μg m⁻³ for the BC_CAWNET forecast, corresponding to an overall error reduction of approximately 17%.

https://doi.org/10.5194/egusphere-2026-1485
Preprint. Discussion started: 20 May 2026

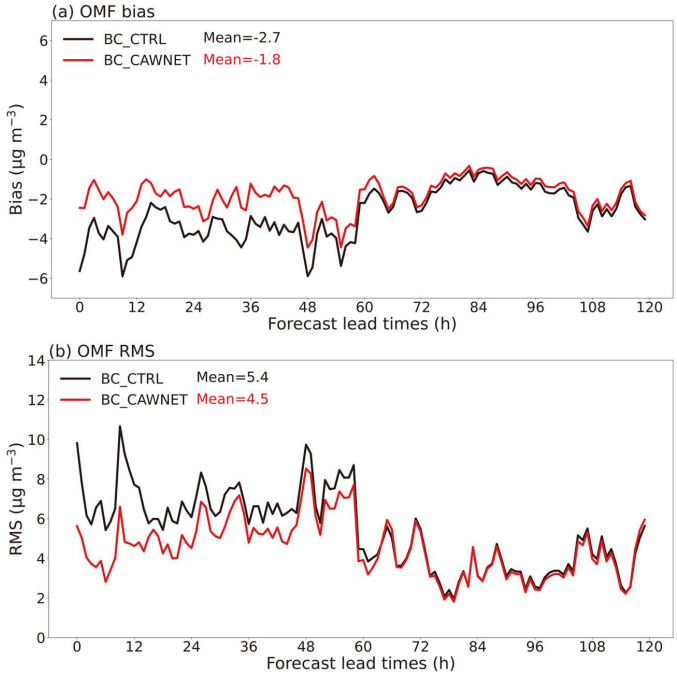

Figure 6. Time series of (a) bias and (b) RMS of BC OMF for BC surface concentrations, spatially averaged over CAWNET stations, for the BC_CTRL and BC_CAWNET forecasts initialized at 00:00 UTC on 19 December 2016.

We further evaluated the BC surface concentration forecast performance of the BC_CTRL and BC_CAWNET experiments over the entire pollution episode using multiple forecast initializations. Figure 7 presents the RMSE improvement of BC_CAWNET forecasts relative to BC_CTRL forecasts for BC surface concentrations throughout the pollution episode. Forecasts were initialized at 00:00 and 12:00 UTC from 16 to 22 December 2016 and verified against CAWNET observations. For both 00:00 and 12:00 UTC initializations, BC_CAWNET forecasts consistently outperform BC_CTRL forecasts throughout the episode. The improvement is most pronounced during the early forecast period (approximately the first 24 h), with the RMSE improvement rate reaching about 20%–50%. As the forecast lead time increases, the RMSE improvement gradually diminishes, and by around 2–3 days, the improvement rate becomes negligible, approaching zero. These results indicate that BC assimilation substantially enhances BC surface concentration forecasts within the first 2–3 days, particularly during the initial forecast stage (e.g., the first 24 h), highlighting its critical role in improving short-range BC prediction during pollution episodes.

https://doi.org/10.5194/egusphere-2026-1485
Preprint. Discussion started: 20 May 2026

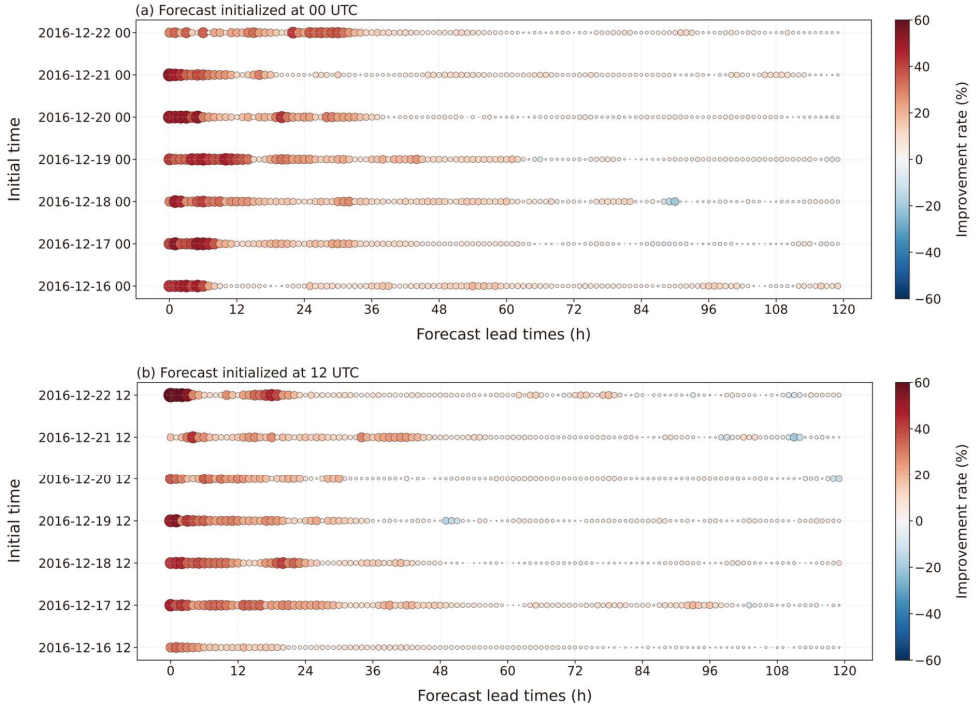

Figure 7. RMSE improvement of BC_CAWNET forecasts relative to BC_CTRL forecasts for BC surface concentrations, initialized at (a) 00:00 UTC and (b) 12:00 UTC during 16–22 December 2016, verified against CAWNET observations.

4.2.2 Impacts on meteorological forecasts

The impacts of BC assimilation on meteorological forecast performance were further assessed using near-surface 2 m air temperature (T2m) as a representative variable. Results from Part 1 of this study (Liu et al., 2025) showed that assimilating BC surface observations produces notable analysis increments in several key meteorological variables, including temperature, pressure, east–west component of horizontal wind, and relative humidity. Since T2m is a diagnostic variable derived from these prognostic fields in the model, it effectively synthesizes the combined influence of BC assimilation on near-surface meteorological conditions. Therefore, T2m is well suited for evaluating the integrated impacts of BC assimilation on meteorological forecast performance. The reference for evaluation is the T2m analysis from the operational CMA-GFS 4D-Var system at the same valid times.

Figure 8 shows the differences in T2m forecasts over eastern China initialized at 00:00 UTC on 19 December 2016 between the BC_CTRL forecasts and the CMA-GFS 4D-Var analysis, the BC_CAWNET forecasts and the CMA-GFS 4D-Var analysis, and between the BC_CAWNET and BC_CTRL forecasts, at forecast lead times of 6, 12, and 24 h. Overall, the spatial patterns in the left and middle columns are highly similar, indicating that the assimilation of BC surface observations does not introduce

https://doi.org/10.5194/egusphere-2026-1485
Preprint. Discussion started: 20 May 2026

adverse impacts on T2m forecasts. Moreover, notable improvements are evident over heavily polluted regions. At 6 h lead time, the BC_CTRL forecasts exhibit a pronounced warm bias of approximately 3 K over region R1 and cold biases of about 4 K over regions R2 and R3 (Fig. 8a). In comparison, the BC_CAWNET forecasts substantially reduce both the warm bias over R1 and the cold biases over R2 and R3, with biases decreasing to about 1 K over R1 and 2–3 K over R2 and R3 (Fig. 8b). Consistently, the differences between the BC_CAWNET and BC_CTRL forecasts show T2m differences of approximately 2 K across these regions, consistent with the reduced biases noted above (Fig. 8c). At 12 h lead time, the BC_CTRL forecasts overestimate T2m by about 3–5 K over region R4 and underestimate it by approximately 2 K over region R5 (Fig. 8d). The BC_CAWNET forecasts reduce the warm bias over R4 to about 2–4 K and weaken the cold bias over R5, with slight warm biases appearing in some areas (Fig. 8e). The direct comparison between the two forecasts further indicates T2m differences of around 1 K over regions R4 and R5 (Fig. 8f). At 24 h lead time, the T2m forecasts from BC_CAWNET and BC_CTRL show largely similar spatial patterns (Figs. 8g, h). Nevertheless, over region R6, the BC_CAWNET forecasts continue to make a positive contribution by further attenuating the cold bias present in the BC_CTRL forecasts, although the magnitude is smaller than 1 K (Fig. 8i). These results demonstrate that the assimilation of BC surface observations does not degrade T2m forecast skill and yields positive impacts over heavily polluted regions. The improvements primarily manifest as a reduction in both warm and cold biases and are most pronounced during the early forecast period, gradually diminishing with increasing forecast lead time.

https://doi.org/10.5194/egusphere-2026-1485
Preprint. Discussion started: 20 May 2026

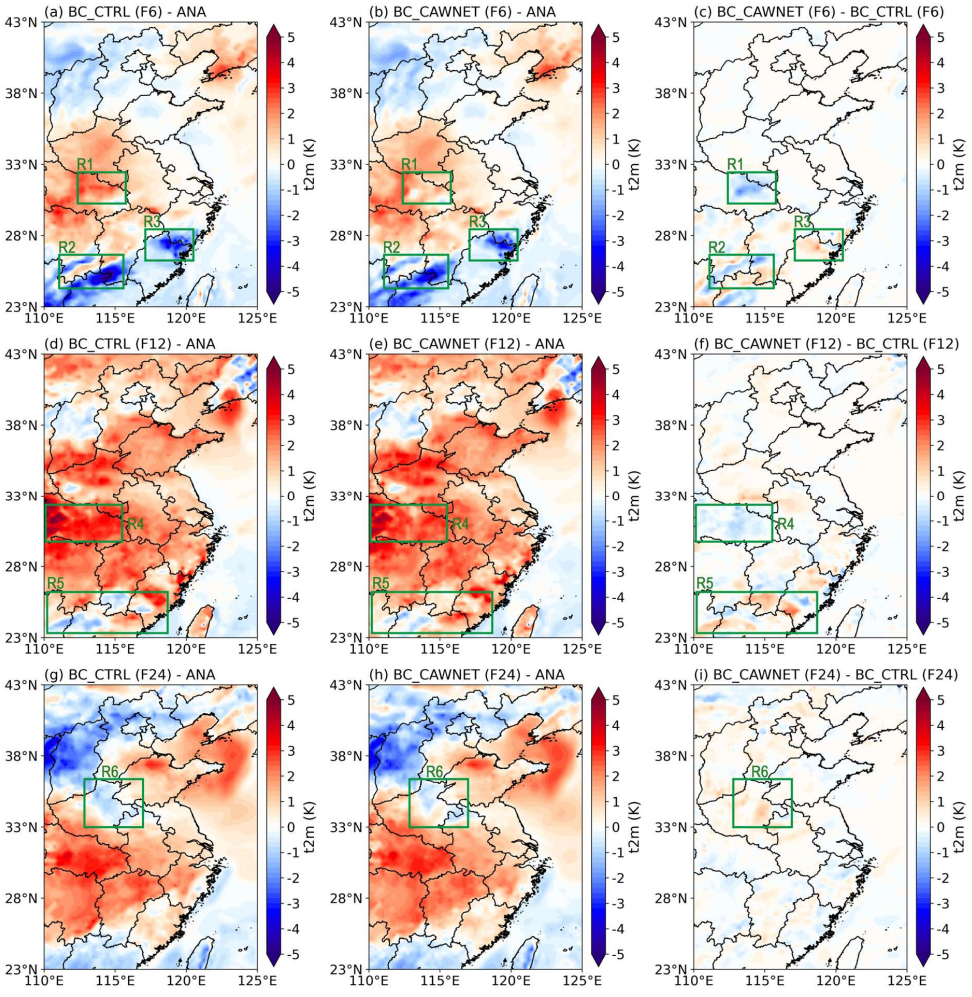

Figure 8. Differences in T2m forecasts over eastern China, initialized at 00:00 UTC on 19 December 2016, between BC_CTRL and the CMA-GFS 4D-Var analysis (left column), BC_CAWNET and the CMA-GFS 4D-Var analysis (middle column), and BC_CAWNET and BC_CTRL (right column), at forecast lead times of 6, 12, and 24 h (from top to bottom).

5 Conclusions

On the basis of the strongly coupled aerosol–meteorology data assimilation system CMA-GFS-AERO 4D-Var developed in Part 1 of this study (Liu et al., 2025), we conducted nearly three months of cycling assimilation experiments with BC surface observations to evaluate the impacts of BC assimilation on the quality of BC background and analysis fields, as well as on BC concentration and meteorological forecasts performance. The results demonstrate that the CMA-GFS-AERO 4D-Var system maintains stability and reliability during the cycling assimilation experiments and is capable of effectively assimilating BC

https://doi.org/10.5194/egusphere-2026-1485
Preprint. Discussion started: 20 May 2026

surface observations, indicating its potential for operational applications. The assimilation of BC surface observations leads to substantial reductions in the BC OMB and OMA values, yielding pronounced improvements in both the background and analysis fields. The resulting BC analyses exhibit a high degree of consistency with the assimilated observations. Independent validation against MERRA-2 reanalysis data further indicates that the inclusion of BC surface observations enhances model constraints and significantly improves the reliability and robustness of the BC analysis fields.

In terms of forecasting performance, BC assimilation markedly improves BC surface concentration forecasts, with more pronounced benefits observed under regional heavy pollution conditions. The forecast improvements are mainly concentrated within the first 2–3 days, with the most substantial enhancement occurring during the initial forecast period (approximately the first 24 h), underscoring the critical role of BC assimilation in short-term pollution forecasting. In addition, the assimilation of BC surface observations exerts a positive influence on near-surface 2 m air temperature forecasts over heavily polluted regions, primarily manifested as a simultaneous reduction in both warm and cold biases. This meteorological impact is most evident during the early forecast period and gradually diminishes with increasing forecast lead time.

Future work will focus on expanding the CMA-GFS-AERO 4D-Var system to assimilate additional aerosol species, such as dust, sulfate, and organic carbon, in order to investigate their synergistic effects on both aerosol and meteorological forecast performance. A broader range of aerosol observations will also be incorporated to support multi-species aerosol assimilation. Furthermore, the system will be applied to optimize control variables, such as emission scaling factors, aiming to improve the analysis and forecast performance of both aerosol and meteorological variables.

https://doi.org/10.5194/egusphere-2026-1485
Preprint. Discussion started: 20 May 2026

Data and code availability. The main components of the CMA-GFS-AERO 4D-Var code are available on Zenodo (Liu et al., 2025, https://doi.org/10.5281/zenodo.14880420). Model outputs from the forecast experiments used in this study are available on Zenodo (Wang et al., 2026, https://doi.org/10.5281/zenodo.18917297).

Author contributions. CW led the writing and analysis of the manuscript. YL conceived the idea and performed the simulations. XZ, XS and WH envisioned and oversaw the project. All authors reviewed the manuscript and provided suggestions on text and figures.

Competing interests. The contact author has declared that none of the authors has any competing interests.

Acknowledgements. This work was supported by the National Natural Science Foundation of China (42305111) and the Major Program of National Natural Science Foundation of China (42090032). The assimilation and forecast experiments were performed on the high-performance computer Pi-SUGON of China Meteorological Administration. The development of the CMA-GFS-AERO 4D-Var system is a collaborative effort involving contributions from many colleagues. We sincerely thank the entire team for their cooperation. We also thank YaQiang Wang from CAMS for providing anthropogenic emission sources data and black carbon observations.

References

Baklanov, A., Schlünzen, K., Suppan, P., Baldasano, J., Brunner, D., Aksoyoglu, S., Carmichael, G., Douros, J., Flemming, J., Forkel, R., Galmarini, S., Gauss, M., Grell, G., Hirtl, M., Joffre, S., Jorba, O., Kaas, E., Kaasik, M., Kallos, G., Kong, X., Korsholm, U., Kurganskiy, A., Kushta, J., Lohmann, U., Mahura, A., Manders-Groot, A., Maurizi, A., Moussiopoulos, N., Rao, S. T., Savage, N., Seigneur, C., Sokhi, R. S., Solazzo, E., Solomos, S., Sørensen, B., Tsegas, G., Vignati, E., Vogel, B., and Zhang, Y.: Online coupled regional meteorology chemistry models in Europe: current status and prospects, Atmos. Chem. Phys., 14, 317–398, https://doi.org/10.5194/acp-14-317-2014, 2014.

Benedetti, A., Morcrette, J. J., Boucher, O., Dethof, A., Engelen, R. J., Fisher, M., Flentje, H., Huneeus, N., Jones, L., Kaiser, J. W., Kinne, S., Mangold, A., Razinger, M., Simmons, A. J., Suttie, M.: Aerosol analysis and forecast in the European Centre for Medium-Range Weather Forecasts Integrated Forecast System: 2. Data assimilation, J. Geophys. Res., 114, D13205, doi:10.1029/2008JD011115, 2009.

Bocquet, M., Elbern, H., Eskes, H., Hirtl, M., Žabkar, R., Carmichael, G. R., Flemming, J., Inness, A., Pagowski, M., Pérez Camaño, J. L., Saide, P. E., San Jose, R., Sofiev, M., Vira, J., Baklanov, A., Carnevale, C., Grell, G., and Seigneur, C.: Data assimilation in atmospheric chemistry models: current status and future prospects for coupled chemistry meteorology models, Atmos. Chem. Phys., 15, 5325–5358, https://doi.org/10.5194/acp-15-5325-2015, 2015.

https://doi.org/10.5194/egusphere-2026-1485
Preprint. Discussion started: 20 May 2026

Bond, T. C., Doherty, S. J., Fahey, D. W., Forster, P. M., Berntsen, T., DeAngelo, B. J., Flanner, M. G., Ghan, S., Kärcher, B., and Koch, D.: Bounding the role of black carbon in the climate system: A scientific assessment, J. Geophys. Res.-Atmos., 118, 5380–5552, https://doi.org/10.1002/jgrd.50171, 2013.

Chen, W., Wang, Y., Li, J., Yi, Z., Zhao, Z., Guo, B., Che, H., and Zhang, X.: Description and evaluation of a newly developed emission inventory processing system (EMIPS), Sci. Total Environ., 870, 161909, https://doi.org/10.1016/j.scitotenv.2023.161909, 2023.

Chung, S. H. and Seinfeld, J. H.: Global distribution and climate forcing of carbonaceous aerosols, J. Geophys. Res.-Atmos., 107, AAC 14-11–AAC 14-33, https://doi.org/10.1029/2001JD001397, 2002.

Engelen, R. J., Serrar, S., and Chevallier, F.: Four-dimensional data assimilation of atmospheric CO2 using AIRS observations, J. Geophys. Res.-Atmos., 114, D03303, doi:10.1029/2008JD010739, 2009.

Gong, S. L., Barrie, L. A., Blanchet, J. P., Von Salzen, K., Lohmann, U., Lesins, G., Spacek, L., Zhang, L. M., Girard, E., and Lin, H.: Canadian Aerosol Module: A size-segregated simulation ofatmospheric aerosol processes for climate and air quality models 1. Module development, J. Geophys. Res.-Atmos., 108, AAC 3-1 – AAC 3-16, https://doi.org/10.1029/2001JD002002, 2003.

Granier, C., Darras, S., Denier van der Gon, H., Doubalova, J., Elguindi, N., Galle, B., Gauss, M., Guevara, M., Jalkanen, J.-P., Kuenen, J., Liousse, C., Quack, B., Simpson, D., and Sindelarova, K.: The Copernicus Atmosphere Monitoring Service Global and Regional Emissions (April 2019 Version), Copernicus Atmosphere Monitoring Service, https://doi.org/10.24380/d0bn-kx16, 2019.

Guerrette, J. J. and Henze, D. K.: Development and application of the WRFPLUS-Chem online chemistry adjoint and WRFDAChem assimilation system, Geosci. Model Dev., 8, 1857–1876, https://doi.org/10.5194/gmd-8-1857-2015, 2015.

Guo, B., Wang, Y., Zhang, X., Che, H., Ming, J., and Yi, Z.: Long-Term variation of black carbon aerosol in China based on revised aethalometer monitoring data, Atmosphere, 11, 684, https://doi.org/10.3390/atmos11070684, 2020.

Inness, A., Baier, F., Benedetti, A., Bouarar, I., Chabrillat, S., Clark, H., Clerbaux, C., Coheur, P., Engelen, R. J., Errera, Q., Flemming, J., George, M., Granier, C., Hadji-Lazaro, J., Huijnen, V., Hurtmans, D., Jones, L., Kaiser, J. W., Kapsomenakis, J., Lefever, K., Leitão, J., Razinger, M., Richter, A., Schultz, M. G., Simmons, A. J., Suttie, M., Stein, O., Thépaut, J.-N., Thouret, V., Vrekoussis, M., Zerefos, C., and the MACC team: The MACC reanalysis: an 8 yr data set of atmospheric composition, Atmos. Chem. Phys., 13, 4073–4109, https://doi.org/10.5194/acp-13-4073-2013, 2013.

Inness, A., Blechschmidt, A. M., Bouarar, I., Chabrillat, S., Crepulja, M., Engelen, R. J., Eskes, H., Flemming, J., Gaudel, A., Hendrick, F., Huijnen, V., Jones, L., Kapsomenakis, J., Katragkou, E., Keppens, A., Langerock, B., de Mazière, M., Melas, D., Parrington, M., Peuch, V. H., Razinger, M., Richter, A., Schultz, M. G., Suttie, M., Thouret, V., Vrekoussis, M., Wagner, A., and Zerefos, C.: Data assimilation of satellite-retrieved ozone, carbon monoxide and nitrogen dioxide with ECMWF's

https://doi.org/10.5194/egusphere-2026-1485
Preprint. Discussion started: 20 May 2026

Composition-IFS. Atmos. Chem. Phys., 15(9), 5275-5303, https://doi.org/10.5194/acp-15-5275-2015, 2015.

Inness, A., Flemming, J., Suttie, M., and Jones, L.: GEMS data assimilation system for chemically reactive gases, ECMWF, 2009.

Janssens-Maenhout, G., Crippa, M., Guizzardi, D., Dentener, F., Muntean, M., Pouliot, G., Keating, T., Zhang, Q., Kurokawa, J., Wankmüller, R., Denier van der Gon, H., Kuenen, J. J. P., Klimont, Z., Frost, G., Darras, S., Koffi, B., and Li, M.: HTAP_v2.2: a mosaic of regional and global emission grid maps for 2008 and 2010 to study hemispheric transport of air pollution, Atmos. Chem. Phys., 15, 11411–11432, https://doi.org/10.5194/acp-15-11411-2015, 2015.

Li, M., Zhang, Q., Kurokawa, J.-I., Woo, J.-H., He, K., Lu, Z., Ohara, T., Song, Y., Streets, D. G., Carmichael, G. R., Cheng, Y., Hong, C., Huo, H., Jiang, X., Kang, S., Liu, F., Su, H., and Zheng, B.: MIX: a mosaic Asian anthropogenic emission inventory under the international collaboration framework of the MICS-Asia and HTAP, Atmos. Chem. Phys., 17, 935–963, https://doi.org/10.5194/acp-17-935-2017, 2017.

Liu, Y., Zhang, X., Han, W., Wang, C., Jia, W., Wang, D., Zhuang, Z., and Shen, X.: Development of the CMA-GFS-AERO 4D-Var assimilation system v1. 0–Part 1: System description and preliminary experimental results. Geosci. Model Dev., 18(15), 4855-4876, https://doi.org/10.5194/gmd-18-4855-2025, 2025.

Mangold, A., De Backer, H., De Paepe, B., Dewitte, S., Chiapello, I., Derimian, Y., Kacenelenbogen, M., Léon, J.-F., Huneeus, N., Schulz, M., Ceburnis, D., O'Dowd, C., Flentje, H., Kinne, S., Benedetti, A., Morcrette, J.-J., and Boucher, O.: Aerosol analysis and forecast in the European Centre for Medium-Range Weather Forecasts Integrated Forecast System: 3. Evaluation by means of case studies. J. Geophys. Res.-Atmos., 116(D3), https://doi.org/10.1029/2010JD014864, 2011.

Ménard, R., Gauthier, P., Rochon, Y., Robichaud, A., de Grandpré, J., Yang, Y., Charrette, C., and Chabrillat, S: Coupled stratospheric chemistry–meteorology data assimilation. Part II: weak and strong coupling. Atmosphere, 10(12), 798, 2019.

Menon, S., Hansen, J., Nazarenko, L., and Luo, Y.: Climate effects of black carbon aerosols in China and India, Science, 297, 2250–2253, https://doi.org/10.1126/science.1075159, 2002.

Randles, C., Da Silva, A., Buchard, V., Colarco, P., Darmenov, A., Govindaraju, R., Smirnov, A., Holben, B., Ferrare, R., and Hair, J.: The MERRA-2 aerosol reanalysis, 1980 onward. Part I: system description and data assimilation evaluation. J. Clim. 30, 6823–6850, https://doi.org/10.1175/JCLI-D-16-0609.1, 2017.

Seinfeld, J. H. and Pandis, S. N.: Atmospheric Chemistry and Physics: From Air Pollution to Climate Change, Environment ence & Policy for Sustainable Development, 1st ed., Wiley-Interscience, New York, https://archive.org/details/atmosphericchemi0000sein (last access: 15 February 2026), 1998.

Semane, N., Peuch, V.-H., Pradier, S., Desroziers, G., El Amraoui, L., Brousseau, P., Massart, S., Chapnik, B., and Peuch, A.: On the extraction of wind information from the assimilation of ozone profiles in Météo–France 4-D-Var operational NWP suite, Atmos. Chem. Phys., 9, 4855–4867, https://doi.org/10.5194/acp-9-4855-2009, 2009.

https://doi.org/10.5194/egusphere-2026-1485
Preprint. Discussion started: 20 May 2026

Xu, X., Yang, X., Zhu, B., Tang, Z., Wu, H., and Xie, L.: Characteristics of MERRA-2 black carbon variation in east China during 2000–2016, Atmos. Environ., 222, 117140, https://doi.org/10.1016/j.atmosenv.2019.117140, 2020.

Zhang, L., Liu, Y., Liu, Y., Gong, J., Lu, H., Jin, Z., Tian, W., Liu, G., Zhou, B., and Zhao, B.: The operational global four-dimensional variational data assimilation system at the China Meteorological Administration, Q. J. Roy. Meteor. Soc., 145, 1882–1896, https://doi.org/10.1002/qj.3533, 2019.

Zhang, Y.: Online-coupled meteorology and chemistry models: history, current status, and outlook, Atmos. Chem. Phys., 8, 2895–2932, https://doi.org/10.5194/acp-8-2895-2008, 2008.

Zheng, B., Tong, D., Li, M., Liu, F., Hong, C., Geng, G., Li, H., Li, X., Peng, L., Qi, J., Yan, L., Zhang, Y., Zhao, H., Zheng, Y., He, K., and Zhang, Q.: Trends in China's anthropogenic emissions since 2010 as the consequence of clean air actions, Atmos. Chem. Phys., 18, 14095–14111, https://doi.org/10.5194/acp-18-14095-2018, 2018.